AMERICAN SOCIETY FOR MICROBIOLOGY | Antimicrobial Agents and Chemotherapy®

ANALYTICAL PROCEDURES

Assessment and Optimizations of *Candida albicans In Vitro* Biofilm Assays

Matthew B. Lohse,[a,b] Megha Gulati,[c] Ashley Valle Arevalo,[c,d] Adam Fishburn,[c] Alexander D. Johnson,[a,e] Clarissa J. Nobile[c]

Department of Microbiology and Immunology, University of California, San Francisco, San Francisco, California, USA[a]; Department of Biology, BioSynesis, Inc., San Francisco, California, USA[b]; Department of Molecular and Cell Biology, School of Natural Sciences, University of California, Merced, Merced, California, USA[c]; Quantitative and Systems Biology Graduate Program, University of California, Merced, Merced, California, USA[d]; Department of Biochemistry and Biophysics, University of California, San Francisco, San Francisco, California, USA[e]

ABSTRACT *Candida albicans* biofilms have a significant medical impact due to their rapid growth on implanted medical devices, their resistance to antifungal drugs, and their ability to seed disseminated infections. Biofilm assays performed *in vitro* allow for rapid, high-throughput screening of gene deletion libraries or antifungal compounds and typically serve as precursors to *in vivo* studies. Here, we compile and discuss the protocols for several recently published *C. albicans in vitro* biofilm assays. We also describe improved versions of these protocols as well as novel *in vitro* assays. Finally, we consider some of the advantages and disadvantages of these different types of assays.

KEYWORDS *Candida albicans*, *in vitro* biofilm assays, biofilm methods, biofilm protocols, biofilm screens, biofilm

Received 29 December 2016 **Returned for modification** 23 February 2017 **Accepted** 3 March 2017

Accepted manuscript posted online 13 March 2017

Citation Lohse MB, Gulati M, Valle Arevalo A, Fishburn A, Johnson AD, Nobile CJ. 2017. Assessment and optimizations of *Candida albicans in vitro* biofilm assays. Antimicrob Agents Chemother 61:e02749-16. https://doi.org/10.1128/AAC.02749-16.

Address correspondence to Clarissa J. Nobile, cnobile@ucmerced.edu.

M.B.L. and M.G. contributed equally to this article.

Candida albicans is a normal part of the human microbiota, but it is also one of only a few fungal species that can cause disease in humans. An important virulence attribute of *C. albicans* is its ability to form biofilms, highly structured communities of cells bound tightly to a surface. In humans, the surface is typically a mucosal or epithelial cell lining, a parenchymal organ, or an implanted medical device, such as a catheter, pacemaker, heart valve, joint prosthesis, or denture. Once formed, these biofilms are resistant to antifungal drugs and also serve as reservoirs that can seed disseminated (nonbiofilm) infections. On the basis of a series of *in vitro* and *in vivo* studies, *C. albicans* biofilm development has been divided into four stages: (i) adherence to a surface, (ii) proliferation on the surface, (iii) maturation into a complex biofilm, and (iv) dispersion of cells from the biofilm to seed new niches (for reviews, see references 1–5).

The past decade has seen the development of several *in vivo* animal models for studying *C. albicans* biofilms (6–12). However, *in vitro* biofilm assays are also critical, as they allow for rapid, high-throughput screening of large deletion libraries and antifungal compounds. They are more ethical and cost-effective than screens carried out directly in an animal model. For example, *in vitro* assays have been used to screen large mutant libraries to identify the genes required for biofilm formation. The findings from these assays were then verified using *in vivo* models (13–21). Likewise, *in vitro* assays have been used as the initial step to identify compounds that inhibit and/or disrupt biofilm formation before the compounds are tested for toxicity in cell culture and in *in vivo* models (22–25). Although there are variations in methodology among the different *in vitro* biofilm assays, at the most basic level they all involve similar steps: initial adherence of cells to a surface coupled with washing to remove nonadhered or weakly adhered cells, followed by a growth step that can vary in length depending on the assay.

Some *in vitro* biofilm assays directly observe biofilms under a microscope, while others use dry weight or optical density (OD) as proxies. For example, a confocal scanning laser microscopy (CSLM) assay examines the architecture of a fluorescently dyed biofilm (or at least that of the parts of the biofilm that the dye can penetrate) (13, 14), and a dry weight (biomass) assay (13, 15, 16, 26) measures the mass of the biofilm. Other assays infer biofilm formation on the basis of measurements of cell viability {e.g., metabolic reduction of the tetrazolium salt reagent 2,3-bis(2-methoxy-4-nitro-5-sulfophenyl)-5-[(phenylamino)carbonyl]-2*H*-tetrazolium hydroxide (XTT) (27, 28) or 3-(4,5-dimethyl-2-thiazolyl)-2,5-diphenyl-2H-tetrazolium bromide (MTT) (29, 30)} or by the uptake of dyes or stains (e.g., crystal violet incorporation into the biofilm [31]). Specialized assays have also been developed to examine specific stages of biofilm development; for example, the number of cells dispersed from an established biofilm can be monitored by CFU counts, hemocytometer counts, and/or optical density measurements (32, 33). Other specialized assays examine factors like growth in a microfluidic chamber (18, 34, 35), active attachment to a surface other than the bottom of a polystyrene plate (34), or the ability of drugs to penetrate into an established biofilm (36).

Although the use of many assays simultaneously would provide the most comprehensive analysis, time limits and financial considerations typically mean that a subset of assays is employed in a given study. The decision to utilize a particular assay is also dependent on the availability of the specific instrumentation needed, such as a confocal microscope for biofilm visualization by CSLM or a flow apparatus for the assessment of biofilm formation in real time. Even when such equipment is available, limits on available time and/or the nature of the experimental setup may impose constraints on the number of conditions that can be evaluated. Another concern is that many assays do not provide information about specific temporal stages of biofilm development or about the resiliency of the biofilm to mechanical disruption. Even differences in the plate format (i.e., 6-, 12-, 24-, 48-, 96-, or 384-well plates) can have an effect. For example, the dry weight and CSLM assays are generally performed in low-density (6-, 12-, or 24-well) formats to provide sufficient material; however, compound testing is often performed in 96- or 384-well plates. The processing of samples for the dry weight and CSLM assays also takes significant time, further reducing the throughput. Some assays involve manipulations of the biofilm, such as washing of the biofilm and addition of a dye, which can result in inadvertent disruptions of the biofilm, thereby confounding the results. Both the careful manipulations needed to reduce this possibility and the larger numbers of replicates used to compensate for any physical disruption that does happen add to the time required for the processing of each sample and reduction of the throughput. The dynamic range of assays can also be an issue; the dry weight assay, for example, is not ideal for detecting enhancements in biofilm formation, as the assay is often saturating. Assays can also introduce biases related to the physical properties of biofilms, such as the failure of a reagent or a dye to penetrate the full depth of the biofilm. Likewise, an assay relying on metabolically active cells (e.g., the XTT reduction assay) may overlook the population of metabolically inactive persister cells commonly found in mature biofilms (37–39). It is also important to note that most *in vitro* biofilm assays are single-endpoint assays, requiring additional replicates to monitor the biofilm over the course of its development.

Recently, we reported on four *in vitro* assays that, together, address some of the issues discussed above. First, we established an assay based on the OD at 600 nm (OD_{600}) to rapidly screen large numbers of conditions and to track the same condition over multiple time points (17, 33, 35). Second, we also developed a new assay to quantitatively determine the number of cells adhering to a surface in the first stage of biofilm development (35). We refer to this assay as the cell adhesion assay. Third, we developed two types of assays (called the standard dispersal assay and the sustained dispersal assay) to quantify cell dispersion at different stages of biofilm development, using only a standard plate reader for analysis (33). Finally, we developed an assay to observe biofilm formation under linear flow in a microfluidic device where adherence

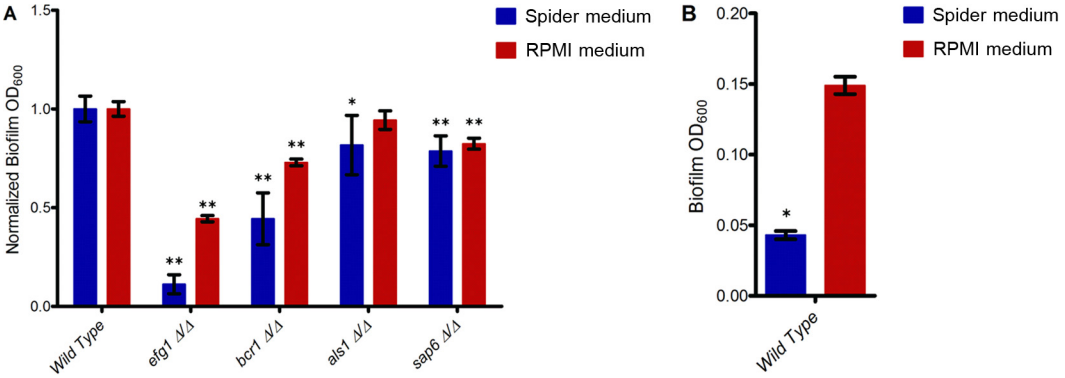

FIG 1 *In vitro* standard optical density assay for biofilm formation in Spider medium and RPMI medium in 384-well microplates after 24 h. (A) The four indicated deletion strains and an isogenic wild-type control strain (SNY250) were adhered to a polystyrene plate for 90 min, unadhered cells were removed, and the remaining cells were allowed to form biofilms for 24 h at 37°C in either Spider or RPMI medium. Biofilm formation was quantified by measuring the OD_{600} of cells that adhered to the bottom of the well after 24 h. Data are the blank-subtracted mean for eight wells per condition normalized to the average for the wild-type strain in the same medium. Error bars represent standard deviations. ** and *, strains that differ from the wild-type strain with significance with *P* values of <0.001 and <0.01, respectively (Student's unpaired *t* test assuming unequal variance). (B) Blank-subtracted, unnormalized OD_{600} measurements of wild-type biofilms grown for 24 h at 37°C in either Spider or RPMI medium. Data are the means for eight wells per condition, and error bars represent standard deviations. *, strains that differ from the wild-type strain in RPMI medium with significance with a *P* value of <0.001 (Student's unpaired *t* test assuming unequal variance).

and cellular morphology can be visually and temporally tracked using time-lapse microscopy throughout the process of biofilm development (35). We refer to this assay as the microfluidic assay. Here, we compile detailed protocols for each of these assays and discuss their advantages and disadvantages.

RESULTS AND DISCUSSION

Optical density assays. We performed 384-well standard optical density assays for four deletion strains (strains with the *efg1*, *bcr1*, *als1*, and *sap6* deletions) that had previously been reported to have various but significant defects in biofilm formation (Fig. 1A) (13, 15, 35, 40). Three of the mutants (the *efg1*, *bcr1*, and *sap6* mutants) differed significantly from the isogenic wild-type strain under both medium conditions tested (RPMI medium and Spider medium). The fourth mutant (the *als1* mutant), in which a more minor biofilm defect was reported in the literature (15, 40), differed significantly from the isogenic wild-type strain under one medium condition (Spider medium) but not under the other (RPMI medium). RPMI medium is more supportive of biofilm formation, resulting in biofilms that are, on average, three times thicker than those grown in Spider medium (Fig. 1B). As a result, the effects of the various mutations are generally more pronounced in Spider medium, and we recommend the use of that medium when looking for more subtle effects.

We performed 384-well optical density inhibition assays for biofilms exposed to antifungal drugs. We used caspofungin and amphotericin B for our assays, as both drugs are known to be effective in preventing biofilm formation. We tested both drugs in the three different inhibition assays; caspofungin (Fig. 2) or amphotericin B (see Fig. S1 in the supplemental material) was added during the 90-min adherence step (adherence inhibition and sustained inhibition assays; panels A and C, respectively, in Fig. 2 and S1) and/or the 24-h growth step (developmental inhibition and sustained inhibition assays; panels B and C, respectively, in Fig. 2 and S1). Both drugs inhibited biofilm formation in each of the three inhibition assay formats. We note, however, that the concentration required for a statistically significant effect (Student's unpaired *t* test assuming unequal variance, $P < 0.001$) or a 50% reduction in biofilm formation (MIC_{50}) in the sustained inhibition assay was sometimes 2- to 4-fold less than the concentration required for similar effects in the other two formats. This is not surprising, as the drug is present during cell adherence as well as biofilm development in the sustained inhibition assay. We also performed 384-well optical density disruption assays for

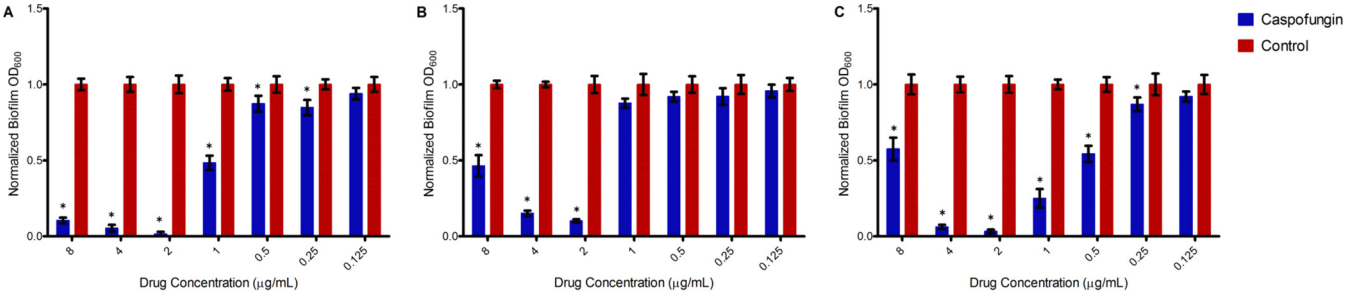

FIG 2 Effects of caspofungin on *in vitro* biofilm formation in three versions of the optical density inhibition assay. A standard wild-type strain (SNY425) was exposed to the indicated concentrations of caspofungin or an equivalent volume of water (control) in the adherence inhibition (A), developmental inhibition (B), and sustained inhibition (C) assays. Biofilm formation was quantified by measuring the OD_{600} of cells adhered to the bottom of the well after 24 h. Data are the blank-subtracted means for eight wells per condition normalized to the average for the water control of the same concentration. Error bars represent standard deviations. *, conditions that differ significantly from the control condition with a *P* value of <0.001 (Student's unpaired *t* test assuming unequal variance).

mature biofilms (24 h) exposed to caspofungin (Fig. 3) or amphotericin B (Fig. S2) for 24 h. Both drugs had effects on the biofilm density, although neither drug resulted in a 50% reduction in biofilm density at any of the concentrations tested, and the magnitude of the effect was less than that seen in any of the inhibition assays. Due to the low standard deviation within all of the optical density assays and the use of eight wells per condition, we could detect statistically significant differences of OD values of $\pm\sim$20% compared to those for the isogenic wild type.

Cell adhesion assay. We performed the 96-well version of the cell adhesion assay with a strain that had previously been reported to have a defect in this assay (a *sap5 sap6* double mutant) (35), a second strain that had a biofilm defect in the standard optical density assay (a *bcr1* mutant) (17), and a third strain that had a biofilm defect *in vivo* in the rat catheter model but that was not previously tested in this assay (an *als1 als3* double mutant) (Fig. 4) (40). All three mutant strains exhibited significantly reduced numbers of cells (measured from the CFU counts) adhering to the well compared to the isogenic wild-type strain. In the case of the *bcr1* mutant strain, the magnitude of the effect observed in this assay (a greater than 90% reduction) was greater than that observed in the standard optical density assay after 24 h of growth (an $\sim$50% reduction; Fig. 1A) or after 90 min of adherence (also an $\sim$50% reduction [17]). As such, the cell adhesion assay may be useful for illuminating more subtle biofilm defects

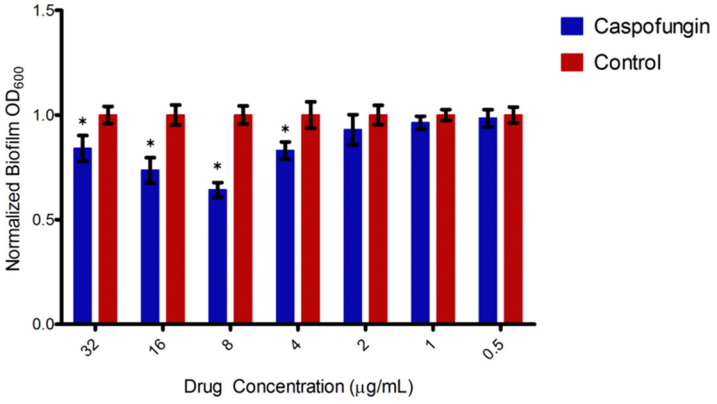

FIG 3 Effects of caspofungin on established biofilms in the optical density disruption assay. Established 24-h biofilms of a standard wild-type strain (SNY425) were exposed to the indicated concentrations of caspofungin or an equivalent volume of water (control) for 24 h. Biofilm disruption was quantified by measuring the OD_{600} of cells that adhered to the bottom of the well at the end of the 24-h exposure period. Data are the blank-subtracted mean for eight wells per condition normalized to the average for the water control of the same concentration. Error bars represent standard deviations. *, conditions that differ significantly from the control condition with a *P* value of <0.001 (Student's unpaired *t* test assuming unequal variance).

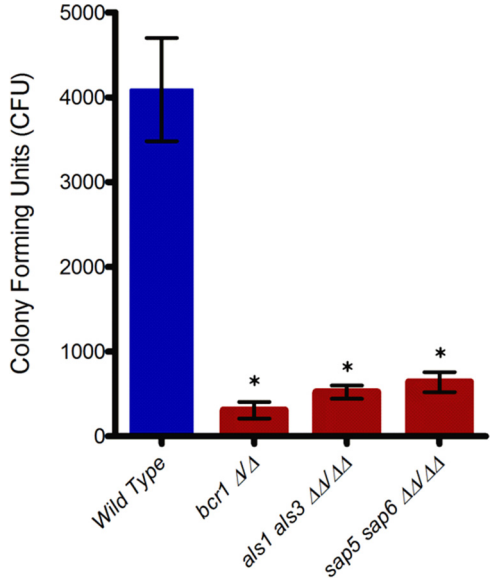

FIG 4 *In vitro* cell adhesion assay. Three deletion strains and an isogenic wild-type control strain (SNY250) were allowed to adhere for 90 min in 96-well plates, and the wells were washed twice with PBS to remove loosely attached cells, following which the remaining cells were vigorously resuspended in water, serially diluted, plated on YPD plates, and grown for 2 days at 30°C before quantification on the basis of CFU counts. Data are the means for 12 wells per strain, and error bars represent standard deviations. *, strains that differ significantly from the control strain with a *P* value of <0.001 (Student's unpaired *t* test assuming unequal variance).

occurring early in the process that might otherwise be overlooked in other assays for biofilm formation, meriting its use, despite the reduced throughput relative to that of the standard optical density assay.

Dispersal assays. We performed both the standard and sustained dispersal assays in a 96-well format with a strain previously reported to have a dispersal defect (an *nrg1* mutant strain) (32). Our results show that, as expected, deletion of *NRG1* results in a significant reduction in the dispersal of cells from biofilms in both the standard (Fig. 5A) and sustained (Fig. 5B) dispersal assays throughout the biofilm life cycle, regardless of nutrient availability.

Microfluidic assay. We performed the microfluidic assay with a wild-type strain under two medium conditions (with RPMI medium and the traditional Spider medium), the same wild-type strain in the presence of the antifungal drug amphotericin B (16

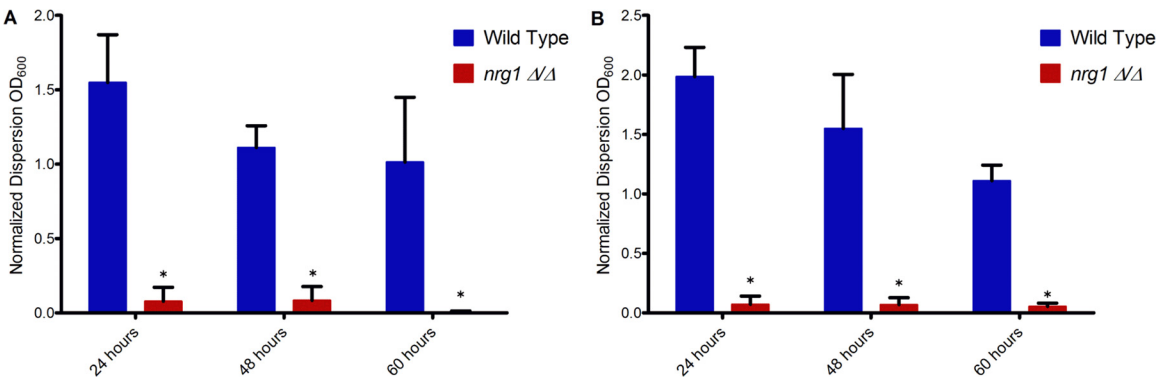

FIG 5 Deletion of *NRG1* results in the reduced dispersal of cells from biofilms in the standard and sustained dispersal assays. The normalized OD_{600}s of medium removed from wells after 24, 48, and 60 h are indicated for isogenic wild-type strain SNY250 and the *nrg1* strain in the standard (A) and sustained (B) dispersal assays. Data are the means for six wells per strain, and error bars represent standard deviations. Dispersion data for each well are normalized on the basis of the OD_{600} of the biofilm in that well at that time point. *, strains that differ significantly from the control strain with a *P* value of <0.001 (Student's unpaired *t* test assuming unequal variance).

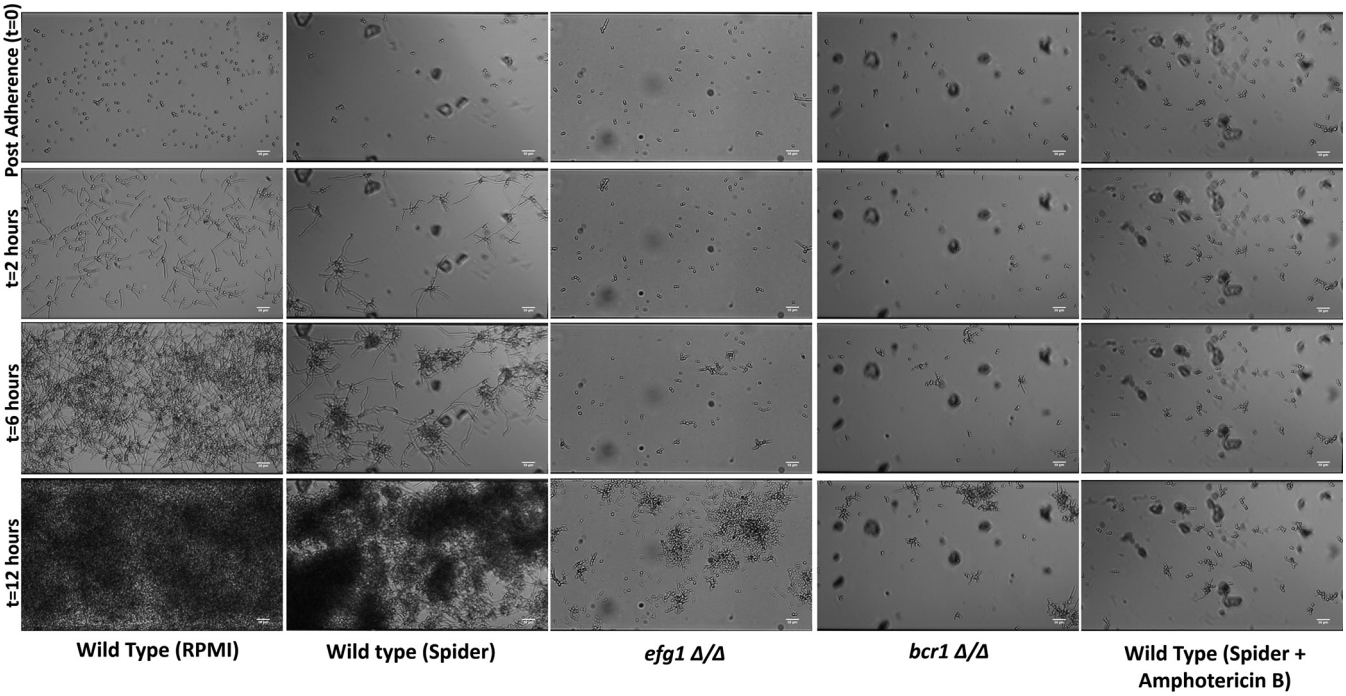

FIG 6 Deletion of either *BCR1* or *EFG1* or exposure to amphotericin B results in biofilm formation defects in the microfluidic assay. The images show the time-dependent visualization of biofilm formation in RPMI medium (column 1), Spider medium (columns 2 to 4), or Spider medium supplemented with 16 μg/ml amphotericin B (column 5) under dynamic flow (0.5 dyne/cm^2) at 37°C for 12 h postadherence in a BioFlux 1000Z microfluidic flow device. Representative images at times (*t*) of 0 h (after adherence and an initial wash), 2 h, 6 h, and 12 h (top to bottom) are shown for isogenic wild-type strain SNY250 (columns 1, 2, and 5), an *efg1* strain (column 3), and a *bcr1* strain (column 4). Bars, 50 μm. Corresponding time-lapse videos of biofilm formation are provided in Videos S1 to S5.

μg/ml), and two strains previously reported to have defects in biofilm formation (*bcr1* and *efg1* mutant strains) (Fig. 6 and Videos S1 to S5) (13, 14, 17). Both of the biofilms formed by the wild-type strain in Spider medium and RPMI medium are dense; however, performance of the assay in RPMI medium results in more cells adhering to the surface and both thicker and faster biofilm formation, as the field of view is completely covered within 10 h. The inclusion of amphotericin B (16 μg/ml) during both the adherence and growth steps had a pronounced effect on adherence, as cells frequently detached from the surface. The inclusion of amphotericin B also resulted in highly reduced hyphal growth and extracellular matrix formation, as the majority of cells were still in the yeast form after 12 h.

In Spider medium, both the *bcr1* and *efg1* deletion strains showed reduced biofilm formation compared to the isogenic wild type; the biofilms of the *bcr1* and *efg1* strains remained sparse even after 12 h of biofilm development. We observed that the *bcr1* yeast cells did not readily adhere to the surface and could be seen to drift away in the direction of medium flow, while the few adhered *bcr1* yeast cells were less developed and formed shorter hyphae than the wild-type strain (Video S4). Unlike the *bcr1* yeast cells, the *efg1* yeast cells showed only slight defects in adherence and hyphal growth, despite the reduced biofilm formation of the *bcr1* mutant relative to the wild type (Video S3). This suggests that the *bcr1* mutant has a cell adhesion defect, which is consistent with our findings in the cell adhesion assay (Fig. 4).

Concluding remarks. There are a wide range of *in vitro* assays for the formation of *C. albicans* biofilms (see Table 1 for a summary), including several not addressed here (e.g., incorporation of ^{3}H-labeled leucine into proteins [26] and the β-1,3 glucan biofilm matrix assay [41, 42]). Even with the more recently developed assays, we still cannot accurately assess certain aspects of biofilm development, especially in a high-throughput manner. Among the underserved areas, we note the need for a matrix assay that detects the α-mannan and/or β-1,6 glucan polysaccharides, which comprise

TABLE 1 Summary of *in vitro* assays discussed in this study as well as other commonly used assays[a]

Technique	Throughput	Specialized equipment required	Works for adherence	Works for dispersal	Advantages	Disadvantages	Reference(s) or source
Cell adhesion	Medium	Plate reader	Yes	No	Minimal sample processing		35, this study
Confocal scanning laser microscopy	Low	Confocal microscope	Maybe	No	Biofilm architecture visualization	Equipment cost, processing time, reagent issues	13, 14
Crystal violet staining	High	Plate reader	Maybe	No		Sample processing can disrupt biofilm, reagent issues	31
Dispersal (flow)	Low-medium	Flow apparatus	No	Yes	Not an endpoint assay	Equipment requirement, no normalization to biofilm thickness	32
Dispersal (standard and sustained)	High	Plate reader	No	Yes	Can normalize to biofilm thickness		33, this study
Dry weight	Low	Analytical balance	Maybe	No		Processing time	13, 15, 16, 26
Microfluidic	Low-medium	BioFlux 1000Z	Yes	No	Not an endpoint assay	Equipment cost	35, this study
Optical density, 96-well format (standard, inhibition, disruption)	High	Plate reader	Maybe	No	Minimal sample processing, no reagent issues	More prone to physical biofilm disruption than 384-well format	17, 33, this study
Optical density, 384-well format (standard, inhibition, disruption)	High	Plate reader	Maybe	No	Minimal sample processing, no reagent issues, less prone to physical biofilm disruption than 96-well format		This study
Silicone square biofilm formation	Medium		Maybe	No			13, 15, 16
XTT or MTT reduction	High	Plate reader	Maybe	No		Sample processing can disrupt biofilm, reagent issues	27–30

[a]The advantages and disadvantages of each are indicated, as well as whether they work for detecting adherence or dispersal and whether they require specialized equipment.

99% of the carbohydrates in the matrix, rather than the relatively minor β-1,3 glucan component (which comprises <1%) detected by the existing assay (43).

Based on our experience with existing *in vitro* biofilm assays, we strongly recommend the optical density assays as an initial screening step for large screens of either mutant libraries or chemical compounds. This recommendation is based on the high throughput and reduced number of processing steps. The cell adhesion, standard dispersal, and sustained dispersal assays offer relatively high-throughput methods for examining specific stages of biofilm development that are not directly apparent from other assays. Most of the assays described here require minimal equipment (a standard plate reader and one or more shaking incubators). The exception is the microfluidic assay, which requires a significant investment (a BioFlux 1000Z microfluidic flow device or equivalent); however, the amount of information that it generates, coupled with its predictive ability for *in vivo* studies, make it the choice (along with CSLM) for following up leads that were generated using the simpler assays.

MATERIALS AND METHODS

Media, reagents, and specialized equipment used. All phosphate-buffered saline (PBS) solutions used in these assays lack calcium and magnesium salts (Dulbecco's PBS, calcium, and magnesium free) and were filter sterilized. Although other media, temperatures, and incubation times can be used for each of the assays described below, the assays were optimized using the media, temperatures, and incubation times indicated below. The cell adhesion assay used RPMI-1640 medium (with L-glutamine, without sodium bicarbonate; catalog number 091060120; MP Biomedicals) supplemented with 34.5 g/liter MOPS (morpholinepropanesulfonic acid; catalog number M3183; Sigma) and adjusted to pH 7.0 using NaOH. The solutions were filter sterilized using a 0.22-μm-pore-size filter and stored at 4°C in the dark pending use. The microfluidic and dispersal (standard dispersal and sustained dispersal) assays used Spider medium (10 g/liter nutrient broth [Difco], 10 g/liter mannitol, 4 g/liter K_2HPO_4, pH 7.2). The optical density assays (standard, adherence inhibition, developmental inhibition, sustained inhibition, and disruption assays) used either RPMI-1640 or Spider medium.

Biofilms were grown under a fixed temperature and shaking conditions using Elmi incubators (Elmi, Ltd., Riga, Latvia); one Elmi incubator can accommodate four plates. Other incubators with equivalent capabilities (e.g., 37°C, 200 to 350 rpm) can also be used. Assays in the 384-well format require specialized multichannel pipettes and pipette tips (Capp) and assay plates that may not be standard laboratory equipment. Deep-well 384-well plates (catalog number P-384-240SQ-C-S; Axygen) can be helpful for prealiquoting solutions into a 384-well format for these assays. The microfluidic assay requires specialized equipment (a BioFlux 1000Z workstation [Fluxion Biosciences]) and plates (BioFlux 48-well low-shear plates [Fluxion Biosciences]). Optical density measurements were made on plate readers with absorbance capabilities (A_{600}) compatible with the 96- and 384-well-plate formats (e.g., a Tecan Infinite M1000 Pro plate reader [Tecan Systems] or a BioTek Epoch 2 plate reader [BioTek Instruments]). Neither fluorescence nor luminescence plate reader capabilities are needed for the assays described below. We note that the area measured by a plate reader may differ from instrument to instrument, and we recommend taking at least five reads from independent locations in each well when working in 96-well formats and taking one read from the center of the well in 384-well formats. For plate readers that measure areas significantly smaller than the wells on a 384-well plate, such as the Tecan Infinite M1000 Pro plate reader, we recommend taking the average of five reads from independent locations in each well, as is done in the 96-well format.

The 96- and 384-well standard optical density biofilm formation assays. The 96- and 384-well optical density assays are derivatives of the previously reported 96-well protocols (17, 33). These assays use flat-bottomed, non-tissue culture-treated 96-well (catalog number 351172; BD Falcon) or 384-well (catalog number 242765; Thermo) plates. For the standard optical density assay, normally used to evaluate biofilm formation by gene deletion mutants, strains are grown at 30°C on YPD (2% Bacto peptone, 2% dextrose, 1% yeast extract) agar plates for 48 h. Overnight cultures are grown overnight in YPD at 30°C either on a roller drum or on a shaker at 250 rpm for 12 to 15 h, cell density is determined in the morning, and cells are added to the wells for a final OD_{600} of 0.5 (equivalent to $\sim 1 \times 10^7$ cells) in 200 μl (for 96-well-plate assays) or 1 μl of an overnight culture in 90 μl (which gives a final OD_{600} of 0.15, equivalent to $\sim 2 \times 10^6$ cells) (for 384-well-plate assays) of RPMI or Spider medium. The plates are then sealed with Breathe-Easy sealing membranes (Diversified Biotech) to reduce evaporation and to prevent cross-contamination between wells. Plates are shaken at 37°C for 90 min at 250 rpm (96-well format) or 350 rpm (384-well format) in an Elmi incubator (Elmi, Ltd., Riga, Latvia), after which the medium is aspirated and the wells are washed with 200 μl (96-well format) or 50 μl (384-well format) 1× PBS, followed by the addition of 200 μl (96-well format) or 90 μl (384-well format) fresh medium. The plates are then resealed and shaken at 37°C for 24 h at 250 rpm (96-well format) or 350 rpm (384-well format) in an Elmi incubator. After 24 h, medium is aspirated from the wells and the optical density (600 nm) is read on a Tecan Infinite M1000 Pro plate reader (Tecan Systems), a BioTek Epoch 2 plate reader (BioTek), or an equivalent standard plate reader. The average density of the reads at five independent locations in each well in a 96-well plate or one read from the center of a 384-well plate is used. Occasionally, an entire well's biofilm will detach during the aspiration step; such outlier wells are noted and excluded from analyses. We note that readings can be taken at time points other than 24 h with this

assay (e.g., after the washes following the adherence step or at the 48-h time point). Both RPMI medium and Spider medium can be used in this assay; RPMI medium normally results in thicker biofilms but can obscure subtle effects more apparent in Spider medium.

For all versions of the optical density assay, data are normalized as follows. The OD_{600} reading of an average blank well is subtracted from the reading of each experimental and control well. The blank-subtracted OD_{600} value of each experimental or control well (normally, eight per condition in the 384-well format and six per condition in the 96-well format) is then normalized to the mean blank-subtracted OD_{600} for the relevant control wells. The standard deviation of each set is then calculated for the normalized data sets, and statistical analyses (normally Student's unpaired two-tailed *t* test assuming unequal variance) are performed.

Inhibition and disruption optical density biofilm formation assays. The inhibition and disruption optical density assays are used for screening antifungal compounds. The 96- and 384-well adherence inhibition, developmental inhibition, and sustained inhibition assays are variations on the standard optical density assay where solutions containing antifungal agents are included during the 90-min adherence step (adherence inhibition and sustained inhibition assays) and/or the 24-h growth step (developmental inhibition and sustained inhibition assays). Different compounds may have different effects in the three inhibition assays; thus, we recommend that all three versions of the assay be performed when practical. If it is feasible to perform only one version of the inhibition assays, we recommend that the sustained inhibition assay be chosen, as it is the most likely to detect an effect.

The 96- and 384-well disruption assays follow the standard optical density assay protocol until the end of the 24-h growth step. At this point, medium is aspirated from the wells (generally in groups of 6 to 12 wells) and 200 μl (96-well format) or 90 μl (384-well format) of medium containing the compound of interest is added to the well. Extreme caution should be taken to avoid touching or otherwise physically disrupting the biofilm during the aspiration or the addition of medium. Fresh medium should be slowly added to the side of the well opposite the side from which medium was aspirated. Medium should be aspirated from and added back to one group of 6 to 12 wells before proceeding to the next group in order to avoid exposing biofilms to air and/or desiccation for extended periods of time. After the disruption step, the plate is resealed and allowed to incubate at 37°C for an additional 24 h at 250 rpm (96-well format) or 350 rpm (384-well format) in an Elmi incubator. After the 24-h postdisruption growth step, medium is aspirated from the wells and the optical density (600 nm) is read as described above for the standard optical density assay protocol.

In general, the 384-well format allows for the screening of more conditions per plate (approximately 45 to 48 for the 384-well format versus 15 to 16 for the 96-well format) in a smaller total volume (720 μl versus 1,200 μl per step), and we prefer it for most screens. The physical (as opposed to chemical) disruption of biofilms occurs much less frequently in the 384-well format than the 96-well format, and as such, we recommend the former approach whenever possible for the disruption assay. We do note, however, that the 96-well format may be preferable in cases where the viscosity of a compound in solution is a consideration. Since a single strain is typically used in the 384-well inhibition or disruption version of the optical density assay, the density of the overnight culture is not determined, and instead, 1 μl of a 12-h overnight culture (approximately 2×10^6 cells) is added to 90 μl medium in each well. We normally use RPMI medium rather than Spider medium for the inhibition and disruption assays.

Advantages and disadvantages of inhibition and disruption optical density biofilm formation assays. The standard optical density assay and its inhibition and disruption variants can be used for the low-volume, high-throughput screening of chemical compound and gene deletion libraries, with more than 40 conditions being able to be evaluated per plate in the 384-well format. It does not require the final washing and dye addition steps of the XTT assay, reducing processing time and costs while avoiding potential complications due to physical disruption of the biofilms. Optical density is also a direct, physical biofilm measurement and thus avoids concerns about incomplete reagent penetrance or concerns about missing the detection of metabolically inactive cells. Since the measurement step does not require the addition of any reagents, the optical density assay can theoretically be combined with the XTT or crystal violet assay by recording the OD_{600} before processing of the wells for those assays. This assay remains an endpoint assay due to the removal of medium prior to recording of the OD_{600}; as such, each well can be used for only one time point and time course experiments require multiple samples. This assay does require a plate reader with 96- and/or 384-well capabilities; however, relatively basic plate readers are capable of filling this role. As this assay provides a direct biofilm measurement rather than a measurement of some proxy for cell viability, we note the theoretical possibility that it could miss the effect of a compound that kills cells in the disruption assay but does not result in the disruption of the biofilm. This assay also does not detect biofilms that might have a structure different from that of normal biofilms, as long as it has the same OD_{600}.

Cell adhesion assay. The cell adhesion assay is based on the protocol initially reported by Winter and colleagues (35) and mimics the adherence step of a 96-well biofilm assay (e.g., the standard optical density assay). Cells are allowed to adhere under standard biofilm-forming conditions ($OD_{600} = 0.5$ [equivalent to 1×10^7 cells] in a 200-μl well volume at 37°C and 250 rpm) for 90 min in 96-well flat-bottomed, non-tissue culture-treated plates (catalog number 351172; BD Falcon). Following the removal of nonadherent cells, the wells are washed twice with 200 μl of PBS. The remaining cells are then vigorously resuspended in water, serially diluted (typically, a 1,000-fold serial dilution of the cells in each well provides an optimal number of cells for counting), plated on YPD plates, and grown for 2 days at 30°C. Cells are then quantified on the basis of CFU counts. In general, we recommend using at least 12 wells per condition for statistical significance.

By measuring the OD_{600} of the wells between the PBS washes and the resuspension step, it is possible to combine this assay with the standard optical density assay. In theory, this assay can be modified to determine the number of viable cells in a biofilm at later time points in a manner similar to that reported by Nailis and colleagues (44). We note, however, that we have been unable to fully break apart *C. albicans* biofilms grown in RPMI medium to isolate single cells, despite trying a number of disruption techniques, all of which caused significant cell death. As such, we recommend careful verification of single cell isolation and cell viability if attempting to modify this protocol to measure cell numbers after the adherence step. If the CFU counts at later stages of biofilm formation are desirable, it is recommended that YNB–1% glucose medium rather than RPMI medium be used since it is easier to break apart biofilms grown in YNB–1% glucose.

Advantages and disadvantages of cell adhesion assay. The cell adhesion assay provides information on a stage of biofilm development that many other assays do not directly quantify. It can be performed for seven conditions (plus a control) per plate. The resuspension, dilution, and plating of cells coupled with the scoring of the number of CFU add to the time and cost of this procedure. As such, it may be worth considering performing the standard optical density assay at the adherence step before proceeding to the cell adhesion assay in order to reduce the number of conditions to screen. This assay also assumes both the consistent homogeneity of cells and equivalent adhesion strengths for different strains during the resuspension process, which may not apply in all cases. Confirmation of the results with a second technique, such as the standard optical density assay or a fluorescence-based assay, may be useful in this case.

Standard and sustained dispersal assays. It has been hypothesized that nutrient availability affects rates of dispersal from biofilms (45). Recent studies have indicated that dispersal rates are increased in rich medium relative to poor or depleted medium (46, 47). The two variants of the dispersal assay described below allow for the comparison between dispersal under nutrient-poor or -exhausted (sustained dispersal) and nutrient-rich (standard dispersal) conditions. These assays are based on a published procedure (33) and have been performed in 6-, 12-, and 96-well-plate formats. We report on the 96-well version here; the protocols for the 6- and 12-well versions are identical except for volume differences (4 ml for 6-well plates, 2 ml for 12-well plates, 200 μl for 96-well plates). The procedure follows the 96-well standard optical density assay protocol until the end of the 24-h growth step. In the standard dispersal assay, 200 μl of medium in each well is removed at the end of the 24-h growth step (taking care not to disturb the biofilm), and the OD_{600} of the removed medium is recorded. Two hundred microliters of fresh medium is then added to the well (again, taking care not to disturb the biofilm), and the biofilm is incubated for a further 24 h, at which point the medium is removed again and the OD_{600} is determined. Fresh medium is once again added, and the biofilms are incubated for a further 12 h before the medium is removed and the OD_{600} is read again. This gives dispersal measurements at the 24-, 48-, and 60-h time points. Normally, five replicate wells are used for each strain. If desired, quantitative CFU counts of the dispersed cells from each assay can be used to compare cell viability between conditions and/or time points.

The sustained dispersal assay varies from the standard dispersal assay in that each set of replicates is viewed at only one of the three time points, rather than after replacement of the growth medium for future reanalysis of the same biofilm. This allows for the quantification of the accumulated biofilm dispersion over the entire 48 or 60 h. Thus, three entirely separate sets of replicates are required to analyze biofilm development at 24, 48, and 60 h.

In order to compensate for normal variation between wells and to allow for comparisons between conditions that result in significant differences in biofilm formation, we recommend that the OD_{600} of each well (after removal of the medium) be determined between the removal and addition of medium at each time point. The dispersal values for each well (OD_{600} or CFU counts) are then normalized to the biofilm OD_{600} for that well.

Advantages and disadvantages of standard and sustained dispersal assays. The standard and sustained dispersal assays can be performed with relatively low volumes (1 ml per step), in a relatively high-throughput manner (15 to 18 conditions per plate), and with minimal manipulation and processing at each time point. These assays eliminate the need for a customized flow apparatus (32) to collect dispersed cells. As mentioned above, the combination of these two assays allows for the evaluation of dispersal under nutrient-rich and -poor conditions. Although we have used 24-, 48-, and 60-h time points, these assays can be easily adapted to examine the results over other time intervals as needed. Furthermore, the ability to normalize to the amount of biofilm present (as determined by the OD_{600}) allows for more accurate comparisons between different conditions and different mutant strains. For example, a mutant strain defective in biofilm formation will have a lower OD value than a wild-type strain, and this can be taken into account when determining the number of cells dispersed by normalization to the OD of each biofilm. In other words, a thinner biofilm generally has fewer cells present and, thus, fewer cells dispersing than a thicker biofilm. However, by normalization directly to the biofilm OD, this dispersal assay can determine if a mutant strain defective in biofilm formation has an increase or a decrease in the number of dispersed cells relative to the number of cells in its biofilm compared to the wild-type strain.

Microfluidic assay. The microfluidic assay allows for the visualization of biofilm formation at a single cell level when the biofilm is exposed to a fixed rate linear flow and is a derivative of the protocol that we previously described (35). This assay uses BioFlux 48-well low-shear plates (Fluxion Biosciences), a BioFlux 1000Z (Fluxion Biosciences) microfluidic flow device, and a Zeiss AX10 microscope. The medium is prewarmed to the desired temperature (normally 37°C) to avoid the formation of bubbles during the experiment. The temperature controller of the system is also set to the desired temperature (normally 37°C). Condensation is removed from the interphase plate before the experiment is set up by running

sterile air through the system at 2 dynes/cm^2 for 10 min. The 48-well low-shear plates (Fluxion Biosciences) are placed in the holder, and 600 to 1,000 μl of medium and/or medium and the compound to be tested are added to the inlet wells (volumes larger than 600 μl are needed for assays over 12 h in length). The interphase plate is then positioned over the 48-well low-shear plates (Fluxion Biosciences) and locked in place so that the system is airtight. Air is removed from the flow wells by running the medium from the inlet to outlet wells for 5 min at 1 dyne/cm^2. Overnight cultures are grown in YPD at 30°C, the density is determined in the morning, and cells are diluted to a final density of an OD_{600} of 0.5 (equivalent to 1×10^7 cells) in 50 μl per well of the desired medium. It is recommended to have three replicates per strain or testing condition. Cells are seeded into the flow cell chamber by adding the cell culture to the outlet well of the BioFlux 48-well plate (Fluxion Biosciences) and running the system with a backward flow (from outlet to inlet) at 2 dynes/cm^2 for 4 s. It is crucial to not exceed 4 s in order to prevent the cells from contaminating the inlet wells. The seeded cells are allowed to adhere with no flow for 20 min at 37°C. Bright-field and phase-contrast prewash images are acquired from three different sections of the flow chamber in each well using a Zeiss AX10 microscope. The wells are then washed with medium flowing from the inlet to the outlet wells at 1 dyne/cm^2 for 5 min to remove nonadherent cells. The remaining cells are incubated at 37°C for 12 h at 0.5 dyne/cm^2. Bright-field and phase-contrast images are acquired from three different sections of the flow chamber in each well every 5 min using a Zeiss AX10 microscope for the remainder of the experiment. The percentage of the area occupied by the biofilm can be quantified using BioFlux Montage software (Fluxion Biosciences).

Advantages and disadvantages of the microfluidic assay. Unlike most *in vitro* biofilm assays, the microfluidic assay allows for the examination of a given sample at a large number of time points. Furthermore, it is customizable for the testing of different temperatures, incubation times, and media and provides information about a number of different aspects of biofilm formation. However, it does require specialized and expensive equipment (BioFlux 1000Z; Fluxion Biosciences) that can process only a limited number of samples (8 conditions/strains in a 48-well plate) in parallel during each 12-h experiment. Despite these limitations, we highly recommend this procedure, as the results, in our experience, have had the best predictive value for *in vivo* biofilm assays compared with those of the other *in vitro* assays that we have assessed.

Working with other *Candida* species. The optical density, cell adhesion, dispersal, and microfluidic assays reported here are optimized for *C. albicans*. In the past, a wide range of *C. albicans* biofilm assays have been used, often with few or no changes, to work with species like *Candida tropicalis*, *Candida parapsilosis*, or *Candida glabrata* (26, 48–54). If the assays reported here are adapted for use with other *Candida* species, be aware that changes in medium and inoculation amounts have been reported to strongly affect multiple aspects of biofilm formation in various species (55). Special care should be taken when comparing results for a given assay across two or more species.

SUPPLEMENTAL MATERIAL

Supplemental material for this article may be found at https://doi.org/10.1128/AAC.02749-16.

SUPPLEMENTAL FILE 1, AVI file, 19.1 MB.
SUPPLEMENTAL FILE 2, AVI file, 13.8 MB.
SUPPLEMENTAL FILE 3, AVI file, 17.2 MB.
SUPPLEMENTAL FILE 4, AVI file, 5.1 MB.
SUPPLEMENTAL FILE 5, AVI file, 13.3 MB.
SUPPLEMENTAL FILE 6, PDF file, 1.0 MB.

ACKNOWLEDGMENTS

We thank all past and present members of the BioSynesis team, the Clarissa J. Nobile lab, and the Alexander D. Johnson lab for helpful discussions on biofilm assay optimizations.

Clarissa J. Nobile and Alexander D. Johnson are cofounders of BioSynesis, Inc., a company developing inhibitors and diagnostics of *C. albicans* biofilms, and Matthew B. Lohse is a consultant of BioSynesis, Inc.

This study was supported by National Institutes of Health (NIH) grants R41AI112038 and R00AI100896 (to C.J.N.) and R01AI083311 (to A.D.J.).

The funders had no role in study design, data collection and interpretation, or the decision to submit the work for publication.

REFERENCES

1. Nobile CJ, Johnson AD. 2015. *Candida albicans* biofilms and human disease. Annu Rev Microbiol 69:71–92. https://doi.org/10.1146/annurev-micro-091014-104330.
2. Gulati M, Nobile CJ. 2016. *Candida albicans* biofilms: development, regulation, and molecular mechanisms. Microbes Infect 18:310–321. https://doi.org/10.1016/j.micinf.2016.01.002.
3. Bonhomme J, D'Enfert C. 2013. *Candida albicans* biofilms: building a heterogeneous, drug-tolerant environment. Curr Opin Microbiol 16:398–403. https://doi.org/10.1016/j.mib.2013.03.007.
4. Douglas LJ. 2003. *Candida* biofilms and their role in infection. Trends Microbiol 11:30–36. https://doi.org/10.1016/S0966-842X(02)00002-1.

5. Kumamoto CA. 2002. *Candida* biofilms. Curr Opin Microbiol 5:608–611. https://doi.org/10.1016/S1369-5274(02)00371-5.
6. Andes D, Nett J, Oschel P, Albrecht R, Marchillo K, Pitula A. 2004. Development and characterization of an *in vivo* central venous catheter *Candida albicans* biofilm model. Infect Immun 72:6023–6031. https://doi.org/10.1128/IAI.72.10.6023-6031.2004.
7. Nett JE, Marchillo K, Spiegel CA, Andes DR. 2010. Development and validation of an *in vivo Candida albicans* biofilm denture model. Infect Immun 78:3650–3659. https://doi.org/10.1128/IAI.00480-10.
8. Nett JE, Brooks EG, Cabezas-Olcoz J, Sanchez H, Zarnowski R, Marchillo K, Andes DR. 2014. Rat indwelling urinary catheter model of *Candida albicans* biofilm infection. Infect Immun 82:4931–4940. https://doi.org/10.1128/IAI.02284-14.
9. Johnson CC, Yu A, Lee H, Fidel PL, Noverr MC. 2012. Development of a contemporary animal model of *Candida albicans*-associated denture stomatitis using a novel intraoral denture system. Infect Immun 80:1736–1743. https://doi.org/10.1128/IAI.00019-12.
10. Řičicová M, Kucharíková S, Tournu H, Hendrix J, Bujdáková H, Van Eldere J, Lagrou K, Van Dijck P. 2010. *Candida albicans* biofilm formation in a new *in vivo* rat model. Microbiology 156:909–919. https://doi.org/10.1099/mic.0.033530-0.
11. Vande Velde G, Kucharíková S, Van Dijck P, Himmelreich U. 2014. Bioluminescence imaging of fungal biofilm development in live animals. Methods Mol Biol 1098:153–167. https://doi.org/10.1007/978-1-62703-718-1_13.
12. Vande Velde G, Kucharíková S, Schrevens S, Himmelreich U, Van Dijck P. 2014. Towards non-invasive monitoring of pathogen-host interactions during *Candida albicans* biofilm formation using *in vivo* bioluminescence. Cell Microbiol 16:115–130. https://doi.org/10.1111/cmi.12184.
13. Nobile CJ, Fox EP, Nett JE, Sorrells TR, Mitrovich QM, Hernday AD, Tuch BB, Andes DR, Johnson AD. 2012. A recently evolved transcriptional network controls biofilm development in *Candida albicans*. Cell 148:126–138. https://doi.org/10.1016/j.cell.2011.10.048.
14. Nobile CJ, Mitchell AP. 2005. Regulation of cell-surface genes and biofilm formation by the *C. albicans* transcription factor Bcr1p. Curr Biol 15:1150–1155. https://doi.org/10.1016/j.cub.2005.05.047.
15. Nobile CJ, Andes DR, Nett JE, Smith FJ, Yue F, Phan QT, Edwards JE, Filler SG, Mitchell AP. 2006. Critical role of Bcr1-dependent adhesins in *C. albicans* biofilm formation *in vitro* and *in vivo*. PLoS Pathog 2:e63. https://doi.org/10.1371/journal.ppat.0020063.
16. Nobile CJ, Nett JE, Andes DR, Mitchell AP. 2006. Function of *Candida albicans* adhesin Hwp1 in biofilm formation. Eukaryot Cell 5:1604–1610. https://doi.org/10.1128/EC.00194-06.
17. Fox EP, Bui CK, Nett JE, Hartooni N, Mui MC, Andes DR, Nobile CJ, Johnson AD. 2015. An expanded regulatory network temporally controls *Candida albicans* biofilm formation. Mol Microbiol 96:1226–1239. https://doi.org/10.1111/mmi.13002.
18. Finkel JS, Xu W, Huang D, Hill EM, Desai JV, Woolford CA, Nett JE, Taff H, Norice CT, Andes DR, Lanni F, Mitchell AP. 2012. Portrait of *Candida albicans* adherence regulators. PLoS Pathog 8:e1002525. https://doi.org/10.1371/journal.ppat.1002525.
19. Nobile CJ, Nett JE, Hernday AD, Homann OR, Deneault JS, Nantel A, Andes DR, Johnson AD, Mitchell AP. 2009. Biofilm matrix regulation by *Candida albicans* Zap1. PLoS Biol 7:e1000133. https://doi.org/10.1371/journal.pbio.1000133.
20. Norice CT, Smith FJ, Jr, Solis N, Filler SG, Mitchell AP. 2007. Requirement for *Candida albicans* Sun41 in biofilm formation and virulence. Eukaryot Cell 6:2046–2055. https://doi.org/10.1128/EC.00314-07.
21. Richard ML, Nobile CJ, Bruno VM, Mitchell AP. 2005. *Candida albicans* biofilm-defective mutants. Eukaryot Cell 4:1493–1502. https://doi.org/10.1128/EC.4.8.1493-1502.2005.
22. Pierce CG, Chaturvedi AK, Lazzell AL, Powell AT, Saville SP, McHardy SF, Lopez-Ribot JL. 2015. A novel small molecule inhibitor of *Candida albicans* biofilm formation, filamentation and virulence with low potential for the development of resistance. NPJ Biofilms Microbiomes 1:15012. https://doi.org/10.1038/npjbiofilms.2015.12.
23. Pierce CG, Saville SP, Lopez-Ribot JL. 2014. High-content phenotypic screenings to identify inhibitors of *Candida albicans* biofilm formation and filamentation. Pathog Dis 70:423–431. https://doi.org/10.1111/2049-632X.12161.
24. LaFleur MD, Lucumi E, Napper AD, Diamond SL, Lewis K. 2011. Novel high-throughput screen against *Candida albicans* identifies antifungal potentiators and agents effective against biofilms. J Antimicrob Chemother 66:820–826. https://doi.org/10.1093/jac/dkq530.
25. LaFleur MD, Sun L, Lister I, Keating J, Nantel A, Long L, Ghannoum M, North J, Lee RE, Coleman K, Dahl T, Lewis K. 2013. Potentiation of azole antifungals by 2-adamantanamine. Antimicrob Agents Chemother 57:3585–3592. https://doi.org/10.1128/AAC.00294-13.
26. Hawser SP, Douglas LJ. 1994. Biofilm formation by *Candida* species on the surface of catheter materials *in vitro*. Infect Immun 62:915–921.
27. Ramage G, Vande Walle K, Wickes BL, López-Ribot JL. 2001. Standardized method for *in vitro* antifungal susceptibility testing of *Candida albicans* biofilms. Antimicrob Agents Chemother 45:2475–2479. https://doi.org/10.1128/AAC.45.9.2475-2479.2001.
28. Nett JE, Cain MT, Crawford K, Andes DR. 2011. Optimizing a *Candida* biofilm microtiter plate model for measurement of antifungal susceptibility by tetrazolium salt assay. J Clin Microbiol 49:1426–1433. https://doi.org/10.1128/JCM.02273-10.
29. Krom BP, Cohen JB, McElhaney-Feser G, Cihlar RL. 2007. Optimized candidal biofilm microtiter assay. J Microbiol Methods 68:421–423. https://doi.org/10.1016/j.mimet.2006.08.003.
30. Krom BP, Cohen JB, McElhaney-Feser G, Busscher HJ, van der Mei HC, Cihlar RL. 2009. Conditions for optimal *Candida* biofilm development in microtiter plates. Methods Mol Biol 499:55–62. https://doi.org/10.1007/978-1-60327-151-6_7.
31. Jin Y, Yip HK, Samaranayake YH, Yau JY, Samaranayake LP. 2003. Biofilm-forming ability of *Candida albicans* is unlikely to contribute to high levels of oral yeast carriage in cases of human immunodeficiency virus infection. J Clin Microbiol 41:2961–2967. https://doi.org/10.1128/JCM.41.7.2961-2967.2003.
32. Uppuluri P, Pierce CG, Thomas DP, Bubeck SS, Saville SP, Lopez-Ribot JL. 2010. The transcriptional regulator Nrg1p controls *Candida albicans* biofilm formation and dispersion. Eukaryot Cell 9:1531–1537. https://doi.org/10.1128/EC.00111-10.
33. Nobile CJ, Fox EP, Hartooni N, Mitchell KF, Hnisz D, Andes DR, Kuchler K, Johnson AD. 2014. A histone deacetylase complex mediates biofilm dispersal and drug resistance in *Candida albicans*. mBio 5:e01201-14. https://doi.org/10.1128/mBio.01201-14.
34. Krom BP, Willems HM. 2016. *In vitro* models for *Candida* biofilm development. Methods Mol Biol 1356:95–105. https://doi.org/10.1007/978-1-4939-3052-4_8.
35. Winter MB, Salcedo EC, Lohse MB, Hartooni N, Gulati M, Sanchez H, Takagi J, Hube B, Andes DR, Johnson AD, Craik CS, Nobile CJ. 2016. Global identification of biofilm-specific proteolysis in *Candida albicans*. mBio 7:e01514-16. https://doi.org/10.1128/mBio.01514-16.
36. Douglas LJ. 2009. Penetration of antifungal agents through *Candida* biofilms. Methods Mol Biol 499:37–44. https://doi.org/10.1007/978-1-60327-151-6_5.
37. Khot PD, Suci PA, Miller RL, Nelson RD, Tyler BJ. 2006. A small subpopulation of blastospores in *Candida albicans* biofilms exhibit resistance to amphotericin B associated with differential regulation of ergosterol and beta-1,6-glucan pathway genes. Antimicrob Agents Chemother 50:3708–3716. https://doi.org/10.1128/AAC.00997-06.
38. LaFleur MD, Kumamoto CA, Lewis K. 2006. *Candida albicans* biofilms produce antifungal-tolerant persister cells. Antimicrob Agents Chemother 50:3839–3846. https://doi.org/10.1128/AAC.00684-06.
39. Honraet K, Goetghebeur E, Nelis HJ. 2005. Comparison of three assays for the quantification of *Candida* biomass in suspension and CDC reactor grown biofilms. J Microbiol Methods 63:287–295. https://doi.org/10.1016/j.mimet.2005.03.014.
40. Nobile CJ, Schneider HA, Nett JE, Sheppard DC, Filler SG, Andes DR, Mitchell AP. 2008. Complementary adhesin function in *C. albicans* biofilm formation. Curr Biol 18:1017–1024. https://doi.org/10.1016/j.cub.2008.06.034.
41. Nett J, Lincoln L, Marchillo K, Massey R, Holoyda K, Hoff B, VanHandel M, Andes D. 2007. Putative role of beta-1,3 glucans in *Candida albicans* biofilm resistance. Antimicrob Agents Chemother 51:510–520. https://doi.org/10.1128/AAC.01056-06.
42. Odabasi Z, Mattiuzzi G, Estey E, Kantarjian H, Saeki F, Ridge RJ, Ketchum PA, Finkelman MA, Rex JH, Ostrosky-Zeichner L. 2004. β-D-Glucan as a diagnostic adjunct for invasive fungal infections: validation, cutoff development, and performance in patients with acute myelogenous leukemia and myelodysplastic syndrome. Clin Infect Dis 39:199–205. https://doi.org/10.1086/421944.
43. Zarnowski R, Westler WM, Lacmbouh GA, Marita JM, Bothe JR, Bernhardt J, Lounes-Hadj Sahraoui A, Fontaine J, Sanchez H, Hatfield RD, Ntambi JM, Nett JE, Mitchell AP, Andes DR. 2014. Novel entries in a fungal

biofilm matrix encyclopedia. mBio 5:e01333-14. https://doi.org/10.1128/mBio.01333-14.
44. Nailis H, Kucharíková S, Ricicová M, Van Dijck P, Deforce D, Nelis H, Coenye T. 2010. Real-time PCR expression profiling of genes encoding potential virulence factors in *Candida albicans* biofilms: identification of model-dependent and -independent gene expression. BMC Microbiol 10:114. https://doi.org/10.1186/1471-2180-10-114.
45. Blankenship JR, Mitchell AP. 2006. How to build a biofilm: a fungal perspective. Curr Opin Microbiol 9:588–594. https://doi.org/10.1016/j.mib.2006.10.003.
46. Sellam A, Al-Niemi T, McInnerney K, Brumfield S, Nantel A, Suci PA. 2009. A *Candida albicans* early stage biofilm detachment event in rich medium. BMC Microbiol 9:25. https://doi.org/10.1186/1471-2180-9-25.
47. Uppuluri P, Chaturvedi AK, Srinivasan A, Banerjee M, Ramasubramaniam AK, Köhler JR, Kadosh D, Lopez-Ribot JL. 2010. Dispersion as an important step in the *Candida albicans* biofilm developmental cycle. PLoS Pathog 6:e1000828. https://doi.org/10.1371/journal.ppat.1000828.
48. Kuhn DM, Chandra J, Mukherjee PK, Ghannoum MA. 2002. Comparison of biofilms formed by *Candida albicans* and *Candida parapsilosis* on bioprosthetic surfaces. Infect Immun 70:878–888. https://doi.org/10.1128/IAI.70.2.878-888.2002.
49. Kuhn DM, George T, Chandra J, Mukherjee PK, Ghannoum MA. 2002. Antifungal susceptibility of *Candida* biofilms: unique efficacy of amphotericin B lipid formulations and echinocandins. Antimicrob Agents Chemother 46:1773–1780. https://doi.org/10.1128/AAC.46.6.1773-1780.2002.
50. Nett J, Lincoln L, Marchillo K, Andes D. 2007. Beta-1,3 glucan as a test for central venous catheter biofilm infection. J Infect Dis 195:1705–1712. https://doi.org/10.1086/517522.
51. Ding C, Butler G. 2007. Development of a gene knockout system in *Candida parapsilosis* reveals a conserved role for *BCR1* in biofilm formation. Eukaryot Cell 6:1310–1319. https://doi.org/10.1128/EC.00136-07.
52. Silva S, Henriques M, Martins A, Oliveira R, Williams D, Azeredo J. 2009. Biofilms of non-*Candida albicans Candida* species: quantification, structure and matrix composition. Med Mycol 47:681–689. https://doi.org/10.3109/13693780802549594.
53. Silva S, Henriques M, Oliveira R, Williams D, Azeredo J. 2010. *In vitro* biofilm activity of non-*Candida albicans Candida* species. Curr Microbiol 61:534–540. https://doi.org/10.1007/s00284-010-9649-7.
54. Estivill D, Arias A, Torres-Lana A, Carrillo-Muñoz AJ, Arévalo MP. 2011. Biofilm formation by five species of *Candida* on three clinical materials. J Microbiol Methods 86:238–242. https://doi.org/10.1016/j.mimet.2011.05.019.
55. Tan Y, Leonhard M, Ma S, Schneider-Stickler B. 2016. Influence of culture conditions for clinically isolated non-*albicans Candida* biofilm formation. J Microbiol Methods 130:123–128. https://doi.org/10.1016/j.mimet.2016.09.011.